Journal of Chromatography A, 1322 (2013) 1–7

Contents lists available at ScienceDirect

Journal of Chromatography A

journal homepage: www.elsevier.com/locate/chroma

Improved performance of micro-fabricated preconcentrators using silica nanoparticles as a surface template

Muhammad Akbar[a,1], Dong Wang[b,1], Ryan Goodman[c], Ashley Hoover[c], Gary Rice[c], James R. Heflin[b], Masoud Agah[a,*]

[a] VT MEMS Lab, Bradley Department of Electrical & Computer Engineering, Virginia Tech, Blacksburg, VA 24061, United States
[b] Department of Physics, Virginia Tech, Blacksburg, VA 24061, United States
[c] Department of Chemistry, The College of William and Mary, Williamsburg, VA 23187, United States

ARTICLE INFO

Article history:
Received 28 August 2013
Received in revised form 27 October 2013
Accepted 28 October 2013
Available online 2 November 2013

Keywords:
Gas chromatography
Micro-thermal preconcentrator
Layer-by-layer self-assembly
Silica nanoparticles
Tenax TA

ABSTRACT

A new approach of enhancing the adsorption capability of the widely used polymer adsorbent Tenax TA poly(2,6-diphenylene oxide) through its deposition on a nano-structured template is reported. The modified Tenax TA-coated silica nanoparticles (SNP) are incorporated as an adsorbent bed in silicon based micro-thermal preconcentrator (μTPC) chips with an array of square microposts embedded inside the cavity and sealed with a Pyrex cover. The interior surface of the chip is first modified by depositing SNP using a layer-by-layer self-assembly technique followed by coating with Tenax TA. The adsorption capacity of the SNP-Tenax TA μTPC is enhanced by as much as a factor of three compared to the one coated solely with thin film Tenax TA for the compounds tested. The increased adsorption ability of the Tenax TA is attributed to the higher surface area provided by the underlying porous SNP coating and the pores between SNPs affecting the morphology of deposited Tenax TA film by bringing nano-scale features into the polymer. In addition, the adsorption ability of the SNP coating as a pseudo-selective inorganic adsorption bed for polar compounds was also observed. The modified Tenax TA-coated SNP μTPC is a promising development toward integrated micro-gas chromatography systems.

1. Introduction

Micro scale gas chromatography (GC) is considered to be one of the leading techniques for the separation and analysis of volatile organic compounds (VOCs). It has a wide range of applications including on-site environmental monitoring, homeland security, and real-time toxic industrial chemicals detection [1–3].

Such systems typically consist of an injector/pre-concentrator, a separation column and a detector all fabricated using microelectromechanical system (MEMS) technology. A MEMS-based thermal pre-concentrator (μTPC) is one of the key components of μGC system for the collection of trace level VOCs in air over a fixed time period to concentrate the analytes before introducing them into a GC column for separation. It consists of an etched cavity in a silicon chip which is filled with adsorbent material. The chip cavity is then sealed by bonding it to another substrate, with heaters and sensors deposited or attached on the backside of the chip afterwards. Analytes are typically desorbed from a μTPC in the form of a sharp sample plug, usually via thermal desorption.

Three different categories of μTPC have been reported in the literature. They are distinguished from each other based on the cavity layout (empty or either encompassing channels or microposts) or by the adsorbent profile (granular or thin film). In the devices using granular adsorbent material, channels and cavities formed in silicon are filled with adsorbent beads and then sealed (bonded) to another substrate [4–11]. The second type of μTPCs utilizes adsorbent materials in the thin film form deposited on a membrane or inside microfabricated channels or cavities [12–18]. There are trade-offs with both types of devices. The first type can provide high sample capacity but suffers from high pressure drops and power consumption during the thermal desorption process. In addition, the difficulty in restricting the beads inside the cavity makes the bonding process extremely cumbersome and can lower the fabrication yield. The devices in the second category significantly reduce the pressure drop, though they have limited sample capacity due to less surface area interacting with the analytes. A third type of μTPC addresses the limitations of the previous types by embedding closely-spaced high-aspect-ratio (HAR) microposts inside an etched cavity and coating them with a thin film adsorbent layer. This approach has been extensively explored and established in our previous work for both enhancing the adsorption capacity and improving the flow distribution in the microchip devices [19–22].

* Corresponding author. Tel.: +1 540 231 2653; fax: +1 540 231 3362.
E-mail address: agah@vt.edu (M. Agah).
[1] These authors contributed equally.

0021-9673/$ – see front matter © 2013 Elsevier B.V. All rights reserved.
http://dx.doi.org/10.1016/j.chroma.2013.10.083

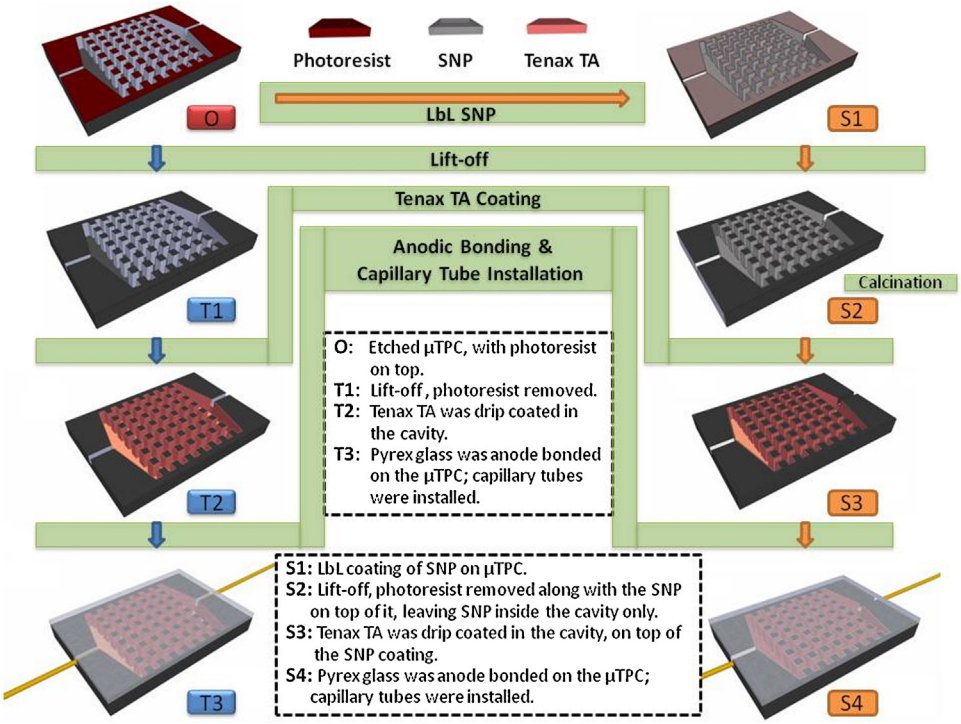

Fig. 1. Fabrication process for μTPCs coated with three different adsorbents. For uncoated μTPC and the one coated with SNP (not shown in the figure), the anodic bonding and capillary tube installation is performed after the lift-off "T1" and calcinations "S2" process, respectively. (For interpretation of the references to color in this text, the reader is referred to the web version of the article.)

There are a variety of commercially available adsorbents for μTPC depending on the chemical properties of VOCs to be concentrated. For example, there is significant literature available on the adsorption properties of Tenax TA in the granular form [23–31], with a few describing the VOCs adsorption mechanisms [32–34]. Our group has published a systematic fundamental study of this polymer in the thin film form with regard to surface topography, crystal structure, thermal stability, modes of adsorption, and adsorption/desorption characteristics [35,36].

Nanotechnology appears to offer the possibility of producing better controlled films which exhibit unique chemistry compared with more established adsorbents. Because of its high thermal stability (up to 800 °C) and large surface area, silica nanoparticle (SNP) coatings would be a good candidate for an adsorbent material, if they could be evenly and conformably deposited on the inner surface of μTPC devices. Very recently, by utilizing the layer-by-layer (LbL) self-assembly technique, our group successfully deposited SNP coatings as a stationary phase for micro GC separation columns [37]. In this paper, we combine the two adsorbents (SNP and Tenax TA) previously used by our group to improve the device performance. The results obtained indicate that the SNP coating as a surface template for Tenax TA polymer can significantly enhance the adsorption capacity of the latter. In addition, the SNP adsorbent alone is found to be able to provide some selectivity in analyte adsorption. These developments provide a novel approach in enhancing the morphology and increasing the surface area of the adsorbent material to improve the overall performance of the μTPC devices.

2. Experimental

2.1. Materials and instruments

Reagent grade VOC compounds, solvents, and Tenax TA (80/100 mesh) used in this work were purchased from Sigma-Aldrich (St. Louis, MO) in >99% purity. Polyallylamine hydrochloride (PAH) and colloid SNP (40–50 nm in diameter, 20–21 wt.% in water) used for LbL deposition were purchased from Sigma-Aldrich (St. Louis, MO) and NISSAN Chemical (Houston, TX) respectively. Single-side polished silicon wafers (4 in., 500 μm thick, n-type) and double-sided polished (4 in., 500 μm thick) Pyrex Wafers were purchased from University Wafers (South Boston, MA). Ultrapure gases (>99% purity) including helium and air were purchase from Airgas (Christiansburg, VA). Fused silica capillary tubing (220 μm outer diameter, 100 μm inner diameter) used as fluidic interfaces were purchased from Polymicro Technologies (Phoenix, AZ). Agilent 5890 and 6890 GC systems used for adsorption/desorption tests and a 30-m long, 320 μm-ID, 0.25 μm film thickness fused silica capillary GC column with dimethypolysiloxane as the stationary phase were purchased from Agilent Technologies, Inc. (Palo Alto, CA). A high performance ceramic heater was purchased from Power Module Inc. (Havertown, PA). Atomic Force Microscopy (Bruker Dimension Icon, ScanAsyst mode) and Field Emission Electron Microscopy (LEO 1550, Zeiss) were used for surface roughness evaluation and imaging purposes respectively.

2.2. μTPC chip fabrication/adsorbent coating

2.2.1. μTPC chip fabrication

The fabrication of μTPC chips starts with the photolithography of micro-posts and fluidic ports using AZ9260 photoresist on a standard 4″ wafer. The wafer is then subjected to deep reactive ion etching (DRIE) to achieve an etching depth of 240 μm. After dicing the etched wafer into individual devices, the chips are ready for adsorbent deposition as described below and in Fig. 1.

2.2.2. Coating thin film Tenax TA

After stripping photoresist with acetone, the etched device was filled with Tenax TA solution (10 mg/ml in dichloromethane) and allowed to evaporate to leave a thin film of the polymer adsorbent

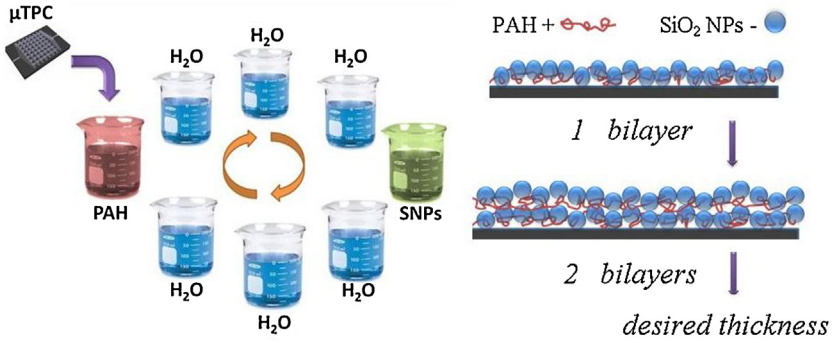

Fig. 2. Schematic procedure of layer-by-layer assembly of SNP coating on μTPC.

on the cavity surfaces. The device is then sealed with a Pyrex 7740 wafer using anodic bonding with temperature, pressure, and voltage set to 320 °C, 22 kPa, and 1250 V, respectively. Finally, fused silica capillary tubes (220 μm O.D. and 100 μm I.D.) are inserted and sealed inside the fluidic channels with epoxy to serve as inlet/outlets for the device, as shown in Fig. 1 (blue "T" process).

2.2.3. Coating SNP

Another alternative adsorbent to Tenax TA which is explored in this study is SNP. Following silicon etching while having photoresist over the un-etched regions, LbL technique [38] was used to coat the interior surfaces of the μTPC with SNPs as shown in Fig. 2. The positively-charged long-chain inert PAH acts like a polymeric "glue" to hold the negatively-charged SNP "bricks" together. The pH of the 10 mM PAH solution and SNP colloid were adjusted to 7.0 (±0.1) and 9.0 (±0.1), respectively, by adding HCl and NaOH solutions in order to achieve maximum surface charge differences for enhancing the electrostatic bonding between the adjacent layers while maintaining colloidal stability.

An automatic dipping system (StratoSequence VI Robot, nanoStrata Inc.) was used to perform the LbL deposition process. Eight beakers were placed in a circle, with one containing PAH solution and another containing SNP colloid. Three beakers were placed between them on each side that could automatically be emptied and refilled with de-ionized (DI) water for rinsing purposes. The μTPC chips, held on glass slides, are first dipped into the PAH solution for 2.5 min, followed by three consecutive one-minute rinsing in DI water. They are then dipped into SNP colloid for another 2.5 min followed by another three rinsing steps before the chips go back into PAH solution. The resulting coating covers the entire surface of the μTPCs, including the internal etched 3D structures and the photoresist left on the top of the chip from the chip fabrication process.

A lift-off procedure via sonication in acetone for 5 min is then used to remove the photoresist along with the SNP coating on top of

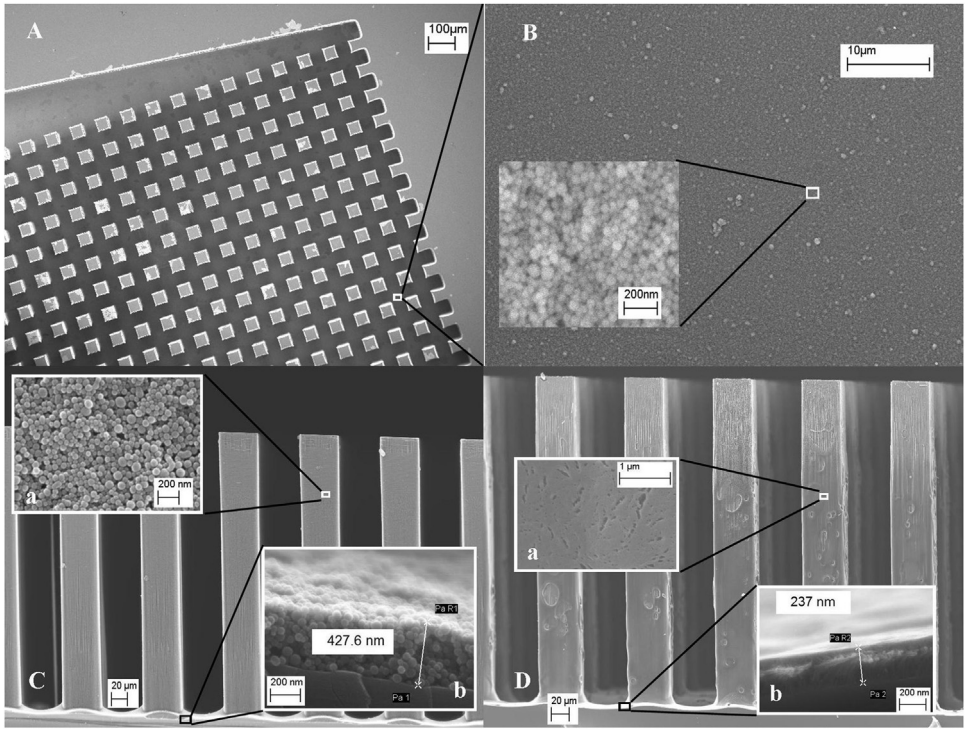

Fig. 3. SEM images of (A) the μTPC coated with 10 BLs SNP (B) top view of the SNP coating on the bottom of the μTPC (C) cross-section view of SNP coating on the sidewall of the micro posts, inset C (a) shows the high magnification view and inset C (b) shows the thickness of SNP coating on the bottom (D) cross-section view of Tenax TA thin film on micro posts, inset D (a) is the closer view of Tenax TA coating on the sidewall of the pillars, inset D (b) shows the thickness of the Tenax TA coating on the bottom of μTPC.

the unetched areas, leaving SNP only on the sidewalls and bottom of the etched features. This process guarantees a smooth clean top surface which is crucial for anodic bonding while in the meantime keeps the SNP coating elsewhere intact. Prior to anodic bonding, the chips were placed in an oven at 500 °C for 4 h. This calcination step removes the PAH and slightly fuses the SNPs together, resulting in a firm SNP coating as the only adsorbent material for the μTPCs. The devices were then sealed by anodic bonding and inlets/outlets installed as previously described in Section 2.2.2.

2.2.4. Coating SNP-Tenax TA

After the SNP calcination step, some of the coated μTPCs were further coated with Tenax TA using the same method previously described. The devices were then sealed by anodic bonding and inlets/outlets installed as previously described in Section 2.2.2. The process is shown in Fig. 1 (orange "S" process).

2.3. Adsorption procedures

All the various chip configurations (SNP, Tenax TA thin film and SNP-Tenax TA) were tested under the same flow conditions (typically 1 ml/min). The sample volumes and injection split ratios were varied to determine the adsorption capacity over a range of polarities using hexane, toluene, 1,2-dichloroethane, and isopropanol as test compounds. Flasks were prepared with septum caps containing each compound and the headspace allowed to become saturated with vapor. For example, assuming ideal gas law behavior, a 1 μl injection of hexane vapor at 1 atm and 25 °C with a 50:1 split injection (1% reaching the μTPC) would be 70 ng. Samples were drawn from the headspace using gas tight syringes and injected immediately into the heated GC injection port. The GC oven was maintained under isothermal conditions at 30 °C. Helium was used as the carrier gas supplied via the GC split/splitless inlet and controlled by the electronic flow controller. The chips were connected directly between the injection port and the flame ionization detector (FID) maintained at 250 °C. The μTPC was mounted on a high performance ceramic heater which was rapidly heated to 250 °C at a ramp rate of ~100 °C/s. A K-type thermocouple coupled to a digital voltmeter was used for manual temperature monitoring and control. After the sample vapor injection, the breakthrough signal (analyte not retained by the preconcentrator) was allowed to return to a baseline level prior to heating for analyte desorption. The ratio of the retained area to total area (unretained plus retained) relative to the total mass injected provides the mass adsorption capacity.

3. Results and discussion

3.1. Theoretical background

The adsorption process of a particular compound on the adsorbent bed depends upon several factors, including the mass of the adsorption bed, the number of available adsorption sites, the flow rate of the carrier gas, the vapor pressures and boiling points of the VOCs, surface area of the adsorbent, and the adsorption temperature.

Different ways of enhancing the surface area have been reported in the literature [19,39–41]. For example, our group has reported [19] the role of different shapes and arrangements of microposts in increasing the surface area. Similarly, another strategy to increase the surface area is to increase the porosity [41] or the surface roughness [22,39]. The current method uses both methods for increasing the surface area by employing an innovative technique of nanoparticle deposition. The μTPC was evaluated in terms of the adsorption capacity and flow rate (resident time) through the chip.

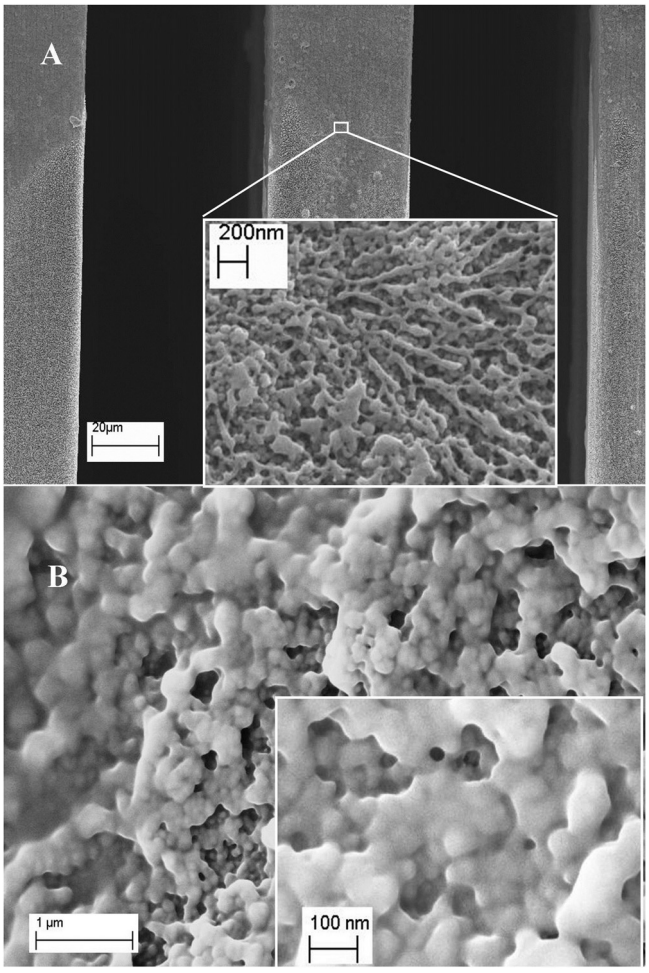

Fig. 4. (A) Cross-section view of Tenax TA coated SNPs on the sidewall of the micro posts, the inset shows the nano-scale structure of Tenax TA brought in by the SNP coating underneath (B) Tenax TA conformably deposited on the SNP template on the bottom.

3.2. Surface characterization of the μTPC chip

FESEM images of the μTPCs with the three different adsorbents (SNP, thin film Tenax TA and SNP-Tenax TA) are shown in Figs. 3 and 4. Fig. 3A–C shows the FESEM images of the μTPC with only SNP as the adsorbent. Fig. 3A shows the top view of the μTPC after the lift-off procedure. A clean top surface is achieved and is beneficial for the anodic bonding process. Meanwhile, the bottom (Fig. 3B) and the sidewall of the microposts (Fig. 3C) are covered with a homogeneous, porous SNP coating (insets of Fig. 3B and C).

The FESEM image of the surface profile of thin film Tenax TA coating in the μTPC is shown in Fig. 3D. Thin film Tenax TA coating on the sidewalls of the microposts experiences low density pores (inset a). From the cross-sectional view of the thin film Tenax TA coating on the bottom, it can be seen the coating has a micro-fiber like structure underneath a dense, relatively smooth surface. Thus, the total available surface area is somewhat limited.

In comparison, the morphology of the Tenax TA coating inside the μTPC was significantly modified by the underlying SNP coating. The FESEM images illustrating this change are shown in Fig. 4. The nanoscaled structure of Tenax TA was developed on the SNP coating present at the sidewall of the microposts. With the help of the SNP coating underneath, the nano "drips" and "strips" Tenax TA fine structure are developed in three dimensions, which significantly increases the surface area of Tenax TA. A different surface morphology of Tenax TA on SNP is achieved on the bottom of the

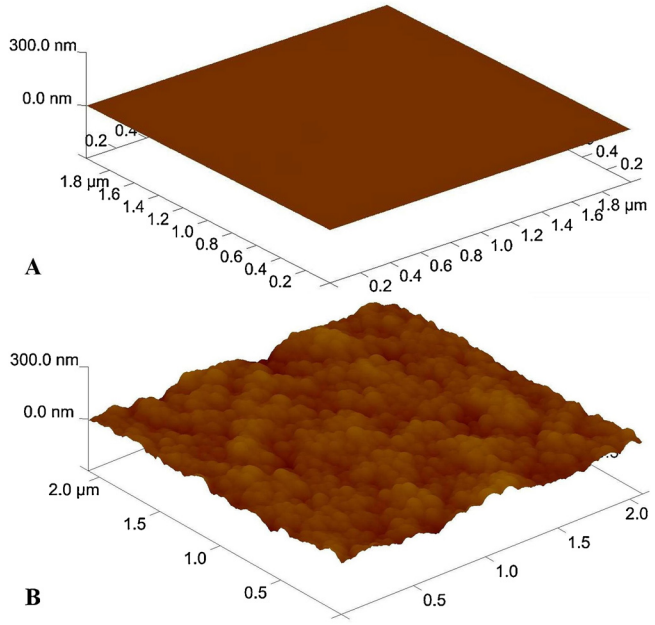

Fig. 5. 3-D AFM image of the surface of (A) silicon wafer surface and (B) 10 bilayers SNP coating on the silicon surface. The analysis was performed on 1 μm × 1 μm chip area.

μTPC, where Tenax TA is conformably coated on the rough surface of the SNP, as shown in Fig. 4B. This may be caused by the different amount of Tenax TA attached to the sidewall of the microposts and the bottom, due to gravitational effects during the Tenax TA deposition and solvent evaporation. This conformal coating could also largely increase the surface area of the Tenax TA by inheriting the large surface area and porosity from SNP coating.

The three dimensional surface profiles of the bare silicon wafer and the 10 bilayers SNP coating on silicon wafer were compared using Atomic Force Microscope (AFM) in Fig. 5. It is quite clear that the roughness, and thus the surface area, is substantially increased by the SNP coating. The measured roughness for a 1 μm × 1 μm area of these two surfaces was around 0.4 nm and 13 nm, respectively, which implies that the surface roughness is increased by a factor of 30. In the case of the Tenax TA coating, the large scale structures limited the use of AFM for measuring the surface roughness. Since the AFM could not probe the real chip due to the fabricated microstructures, the surface measurements were all performed on a planar surface prepared using the same procedure.

3.3. Adsorption capacities

Assuming ideal gas law behavior, the mass amount of analyte injected from a saturated vapor above the pure liquid can be calculated from the injection volume and the split ratio used for the injection. The mass retention of the chips can then be determined from the fraction of the total area retained relative to the total area (breakthrough peak plus retained peak). In this study, the capacity of the devices were initially characterized with μl volumes of analyte sampled from a saturated headspace using gas tight syringes. An example of a typical retention profile for toluene using an SNP-Tenax TA chip is shown in Fig. 6 for three replicate runs. Tailing from the excess hexane in the breakthrough peak is expected due to the porous nature of the SNP layers coupled with weak intermolecular adsorption of multiple analyte layers from oversaturation of the chip; however, the thermal desorption of the trapped hexane at ca. 250 °C was very sharp (w_b < 6–8 s; where w_b represents width of the peak at the base) as well as reproducible over multiple firings. This is a very desirable attribute and necessary for efficient

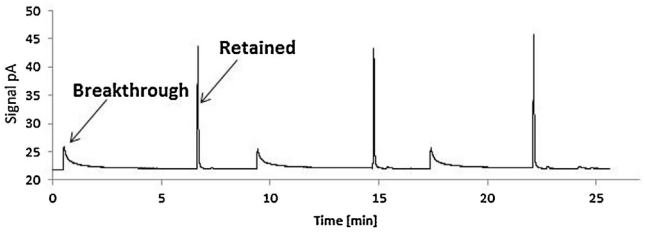

Fig. 6. Triplicate desorption profiles for hexane from an SNP-Tenax TA μTPC.

transfer of analytes as a narrow band to a chromatographic column for separations.

Comparisons of the adsorption capacities for the three types of μTPC chips used are graphically depicted in Fig. 7. All the chips were tested under identical conditions with respect to adsorption temperature (30 °C), flow rate (1 ml/min), and desorption temperature (~250 °C). The adsorption capacity of the SNP-Tenax TA relative to the Tenax TA chip improved by factors of 2.7, 1.3, 1.4, and 3.0 for hexane, toluene, 1,2-dichloroethane, and isopropanol respectively, which represents a range of polarities. The enhanced surface area and morphology of Tenax TA most likely result in these enhancements for low to medium polarity compounds.

The most striking impact from polarity was observed for the SNP chip. Virtually no hexane (a very non-polar compound) was retained by the SNP chips; however, substantially more isopropanol was retained than for either the Tenax TA and SNP-Tenax TA chips (by factors of 9.0 and 3.0 respectively). This is due to the large number of active hydroxyl sites present on the silica surface that will have very strong intermolecular attractions via hydrogen bonding to very polar compounds such as alcohols. The reduced capacity for isopropanol in the presence of Tenax TA is most likely the result of a significant number of these sites being covered by the Tenax TA film. This type of interaction could be advantageous for producing pseudo-selective chips for retention of polar compounds; however additional studies must be performed to ascertain whether

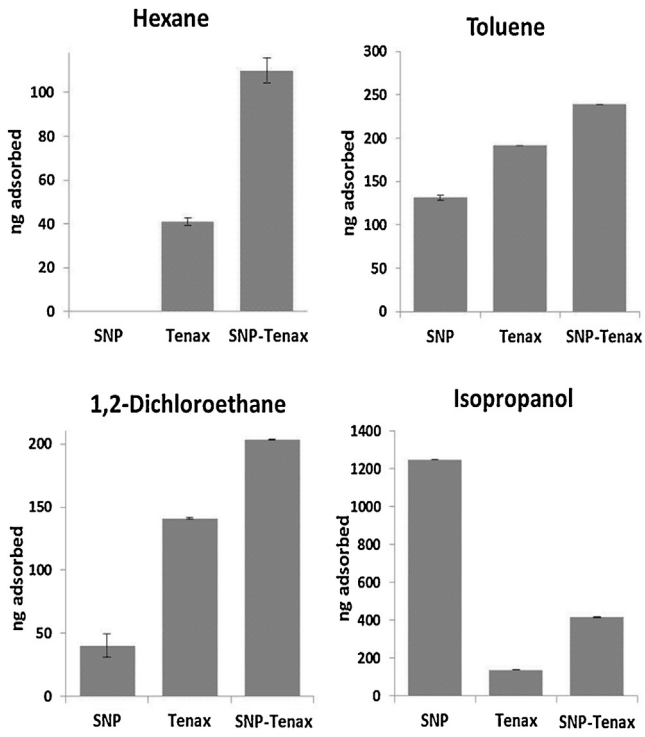

Fig. 7. Adsorption capacities of SNP, Tenax TA, and SNP-Tenax TA μTPCs for hexane, toluene, 1,2-dichloroethane, and isopropanol.

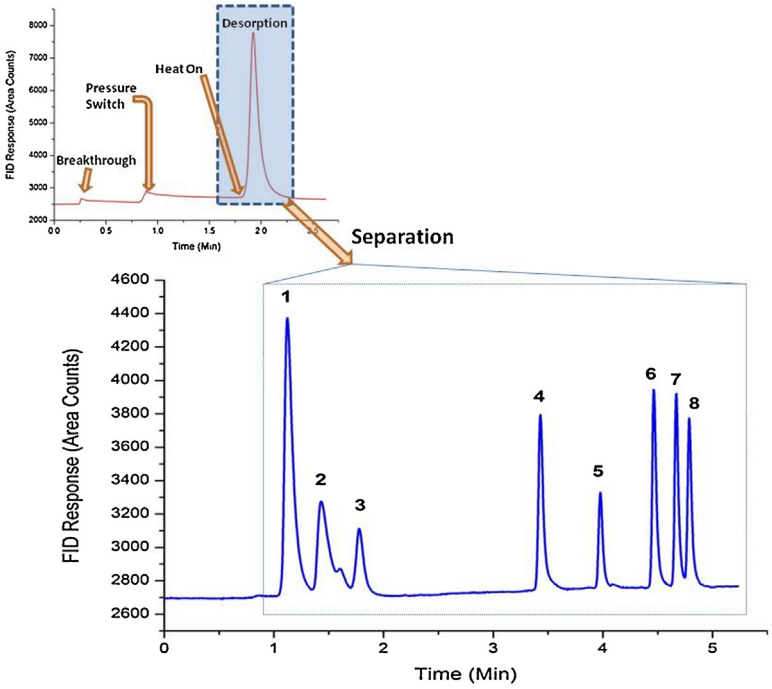

Fig. 8. The performance of the μTPC with SNP-Tenax TA chip for eight VOCs. Adsorption conditions: 5 psi and 10:1 split injection ratio. Desorption conditions: 20 psi and temperature programming (30 °C–15 °C/min–90 °C). Compound identification: (1) chloroform, (2) isopropanol, (3) 1-propanol, (4) toluene, (5) tetrachloroethylene, (6) chlorobenzene, (7) ethylbenzene and (8) p-xylene.

irreversible adsorption could occur with more active polar compounds such as phenols or amines.

The capturing ability of the SNP-Tenax TA chip coupled with a chromatographic separation was successfully demonstrated by testing a mixture of eight commonly found VOCs. The liquid volumes of the VOCs used to produce the mixture were based on the relative vapor pressures of each VOC such that the vapor state mix contained comparable mole amounts of each VOC, assuming ideal gas law conditions. The mixture was contained within a septum sealed bottle. During the adsorption phase, the chip was loaded with a 10 μl headspace volume of the mixture using a gas tight syringe. The pressure was maintained at 5 psi (0.5 ml/min flow rate) to allow sufficient interaction between the analytes and the adsorbent. Before the thermal desorption, the pressure was increased to 20 psi (1.5 ml/min flow rate) and the signal was allowed to return to original level. The increased pressure was necessary to produce an adequate flow rate in the 30-m GC column. In addition, this assists in producing a narrower plug during the thermal desorption process for subsequent separation by increasing the volumetric flow rate. The GC column was then coupled to μTPC and the chip was quickly heated to 250 °C to desorb the compounds. The chromatogram in Fig. 8 is the result of coupling the μTPC to the GC column. It is evident from the chromatogram that the last few peaks widths (compounds 4–8) are significantly narrower than the preceding ones (compounds 1–3). This is due to the condensation of less volatile compounds onto the beginning of the cold GC column after thermal desorption resulting in a narrower sample plug. On the other hand, the more volatile compounds may tend to remain in the vapor phase and continue through the column, resulting in a broader peak width that is based on the desorption characteristics of the μTPC. The results shown in the top inset of Fig. 8 indicate that the chip successfully captured/concentrated all of the injected analytes from the mixture with a desorption peak width of ~10 s and a negligible breakthrough peak, which was expected since the volume injected and split ratio used were comparable to the conditions used for testing the adsorption capacities of the individual compounds previously described. Chromatograms obtained from multiple injections were highly reproducible.

4. Conclusion

A novel approach for enhancing the adsorption capacity of Tenax TA-coated μTPCs using nanoparticle deposition as a surface template has been demonstrated. A promising improvement was attained under similar conditions over ones coated only with thin film Tenax TA. The better capturing ability is attributed to the larger surface area provided by the SNP coating, thus increasing the interaction of gas molecules with the adsorbent surface. The exception to these observations was with a very polar compound, which was pseudo-selectively adsorbed with much higher retention on the SNP chip.

5. Future work

In future work, we envision incorporating the LbL technique to deposit other nanoparticles, such as lead sulfide (PbS), titanium dioxide (TiO_2) or cadmium sulfide (CdS) as reported in Kotov et al. work [42] and investigate their impact on the performance of μTPCs. The thickness, and thus, the number of bilayers of adsorbent may play a vital role in this regard. Additional work will focus on optimizing the number of bilayers to accommodate the best performance of the device for both adsorption and desorption phases. In addition, both surface area and intra-granular porosity can be controlled by changing the size and shape of SNPs. The current study has utilized SNPs with an average diameter of 40–50 nm. There are other types of commercially available SNPs with 20–30 nm and 70–100 nm average diameters [43] that can be explored for adsorption performance. Functionalized nanoparticles could also provide a unique opportunity for selective adsorption of species of interest as well. The capacity of the devices in this study were characterized with μl volumes of analyte sampled from a saturated headspace using gas tight syringes. The same amounts when diluted into a

larger volume (to simulate trace level concentrations) and sampled using a micro-flow pump for testing devices under actual environmental conditions will be considered in future studies [2,44].

Acknowledgements

This research has been supported by the National Science Foundation under Award No. CBET-0854242. All the FESEM images are taken at Virginia Tech Institute for Critical and Applied Science, Nano Scale Characterization and Fabrication Laboratory (ICTAS-NCFL). AFM images were obtained with the help from Mr. Moataz Bellah. Fabrication of the devices was performed at Virginia Tech Microfabrication Cleanroom Facilities.

References

[1] J.H. Seo, S.K. Kim, E.T. Zellers, K. Kurabayashi, Lab Chip 12 (2012) 717.
[2] S.K. Kim, H. Chang, E.T. Zellers, Anal. Chem. 83 (2011) 7198.
[3] J.H. Seo, J. Liu, X. Fan, K. Kurabayashi, Anal. Chem. 84 (2012) 6336.
[4] H.K.L. Chan, S.W. Pang, R.A. Veeneman, E.T. Zellers, M. Takei, The 13th International Conference on Solid-State Sensors, Actuators and Microsystems, vol. 2, 2005, p. 2091.
[5] I. Gràcia, P. Ivanov, F. Blanco, N. Sabaté, X. Vilanova, X. Correig, L. Fonseca, E. Figueras, J. Santander, C. Cané, Sens. Actuators B 132 (2008) 149.
[6] T. Wei-Cheng, H.K.L. Chan, L. Chia-Jung, S.W. Pang, E.T. Zellers, J. Microelectromech. Syst. 14 (2005) 498.
[7] T. Wei-Cheng, S.W. Pang, L. Chia-Jung, E.T. Zellers, J. Microelectromech. Syst. 12 (2003) 264.
[8] A.B. Alamin Dow, W. Lang, Sens. Actuators B 151 (2010) 304.
[9] E.H.M. Camara, P. Breuil, D. Briand, N.F. de Rooij, C. Pijolat, Anal. Chim. Acta 688 (2011) 175.
[10] A. Rydosz, W. Maziarz, T. Pisarkiewicz, K. Domański, P. Grabiec, Microelectron. Reliab. 52 (2012) 2640.
[11] H. Vereb, B. Alfeeli, A. Dietrich, M. Agah, IEEE Sens. (2011) 1237.
[12] M. Kim, S. Mitra, J. Chromatogr., A 996 (2003) 1.
[13] E.W. Simões, S.G. de Souza, M.L.P. da Silva, R. Furlan, H.E. Maldonado Peres, Sens. Actuators B 115 (2006) 232.
[14] I. Voiculescu, R.A. McGill, M.E. Zaghloul, D. Mott, J. Stepnowski, S. Stepnowski, H. Summers, V. Nguyen, S. Ross, K. Walsh, M. Martin, IEEE Sens. J. 6 (2006) 1094.
[15] C.E. Davis, C.K. Ho, R.C. Hughes, M.L. Thomas, Sens. Actuators B 104 (2005) 207.
[16] G.C. Frye-Mason, R.P. Manginell, E.J. Heller, C.M. Matzke, S.A. Casalnuovo, V.M. Hietala, R.J. Kottenstette, P.R. Lewis, C.C. Wong, International Conference on Microprocesses and Nanotechnology. Microprocesses and Nanotechnology' 99, 1999, p. 60.
[17] M. Martin, M. Crain, K. Walsh, R.A. McGill, E. Houser, J. Stepnowski, S. Stepnowski, H.-D. Wu, S. Ross, Sens. Actuators B 126 (2007) 447.
[18] P.R. Lewis, P. Manginell, D.R. Adkins, R.J. Kottenstette, D.R. Wheeler, S.S. Sokolowski, D.E. Trudell, J.E. Byrnes, M. Okandan, J.M. Bauer, R.G. Manley, C. Frye-Mason, IEEE Sens. J. 6 (2006) 784.
[19] B. Alfeeli, M. Agah, IEEE Sens. J. 11 (2011) 2756.
[20] B. Alfeeli, D. Cho, M. Ashraf-Khorassani, L.T. Taylor, M. Agah, Sens. Actuators B 133 (2008) 24.
[21] M. Akbar, M. Agah, 2012 IEEE 25th International Conference on Micro Electro Mechanical Systems (MEMS), 2012, p. 906.
[22] M. Akbar, M. Agah, J. Microelectromech. Syst. 22 (2013) 443.
[23] E.D. Pellizzari, J.E. Bunch, R.E. Berkley, J. McRae, Anal. Lett. 9 (1976) 45.
[24] R.H. Brown, C.J. Purnell, J. Chromatogr. 178 (1979) 79.
[25] S. Seshadri, J.W. Bozzelli, Chemosphere 12 (1983) 809.
[26] I. Maier, M. Fieber, J. High Resolut. Chromatogr. 11 (1988) 566.
[27] K. Ventura, M. Dostál, J. Churácek, J. Chromatogr. 642 (1993) 379.
[28] V. Simon, M.-L. Riba, A. Waldhart, L. Torres, J. Chromatogr., A 704 (1995) 465.
[29] A. Kroupa, J. Dewulf, H. Van Langenhove, I. Viden, J. Chromatogr., A 1038 (2004) 215.
[30] R. Borusiewicz, J. Zieba-Palus, J. Forensic Sci. 52 (2007) 70.
[31] M. Schneider, K.-U. Goss, Anal. Chem. 81 (2009) 3017.
[32] K. Sakodynskii, L. Panina, N. Klinskaya, Chromatographia 7 (1974) 339.
[33] D. Zhao, J.J. Pignatello, Environ. Toxicol. Chem. 23 (2004) 1592.
[34] A. Alentiev, E. Drioli, M. Gokzhaev, G. Golemme, O. Ilinich, A. Lapkin, V. Volkov, Y. Yampolskii, J. Membr. Sci. 138 (1998) 99.
[35] B. Alfeeli, V. Jain, R.K. Johnson, F.L. Beyer, J.R. Heflin, M. Agah, Microchem. J. 98 (2011) 240.
[36] B. Alfeeli, L.T. Taylor, M. Agah, Microchem. J. 95 (2010) 259.
[37] D. Wang, H. Shakeel, J. Lovette, G.W. Rice, J.R. Heflin, M. Agah, Anal. Chem. 85 (2013) 8135.
[38] G. Decher, Science 277 (1997) 1232.
[39] S. Xu, S. Hartvickson, J.X. Zhao, ACS Appl. Mater. Interfaces 3 (2011) 1865.
[40] H. Föll, M. Christophersen, J. Cartensen, G. Hasse, Mater. Sci. Eng., R 39 (2002) 93.
[41] E.H.M. Camara, P. Breuil, D. Briand, L. Guillot, C. Pijolat, N.F. de Rooij, Sens. Actuators B 148 (2010) 610.
[42] N.A. Kotov, I. Dekany, J.H. Fendler, J. Phys. Chem. 99 (1995) 13065.
[43] J. Ho, W. Zhu, H. Wang, G.M. Forde, J. Colloid Interface Sci. 308 (2007) 374.
[44] T. Sukaew, H. Chang, G. Serrano, E.T. Zellers, Analyst 136 (2011) 1664.